ELSEVIER

Journal of Power Sources 88 (2000) 237–242

JOURNAL OF POWER SOURCES

www.elsevier.com/locate/jpowsour

# Characterization of a commercial size cylindrical Li-ion cell with a reference electrode

Qunwei Wu, Wenquan Lu, Jai Prakash *

*Department of Chemical and Environmental Engineering, Center for Electrochemical Science and Engineering, Illinois Institute of Technology, 10 W 33rd Street, Chicago, IL 60616, USA*

Received 8 November 1999; accepted 16 December 1999

**Abstract**

A method of monitoring the performance of the cell components was developed to study the cycling behavior of the commercial size rechargeable lithium-ion cells. A lithium reference electrode was placed into the center of a full commercial cylindrical cell in an effort to monitor the electrochemical behavior of the cell and its component electrodes during cycling. This technique allowed the resolution of measured voltage into component cathode and anode voltages and hence the resolution of the total area-specific impedance (ASI) into cathode and anode ASI. The cathode was found to be the electrode limiting the power and capacity of the Li-ion cell. Further investigations also revealed that the increase in the cathode ASI is a main cause of power and energy degradation of the cell during cycling. 

*Keywords:* Lithium-ion batteries; Reference electrode; Lithium cobalt oxide; Area specific impedance

## 1. Introduction

Ambient lithium-ion rechargeable batteries that are based on rocking chair concept [1] have high energy density. Therefore, they are attractive for portable electronic device and electric vehicle applications [2,3]. Indeed, a first generation of cylindrical and prismatic design Li-ion cells is being used in cellular telephones and laptop computers. Yet, intense research and development efforts are continuing to improve the performance and safety characteristics of these batteries.

The Li-ion battery chemistry is based on $LiMO_2$ (where M = Mn, Ni, Co and their combinations) as cathode material and graphite as the negative material. The kinetics and mechanisms of the electrode reactions are controlled by the interfacial properties between the solid-state electrodes and the liquid organic electrolyte. During cycling, a combination of electrode polarization, ohmic drop, $Li^+$ diffusion through the electrolyte, and solid-state diffusion within the electrode cause the overall cell voltage to change. These changes should be kept as low as possible in order to reach the highest power and energy output. Monitoring the performance of both positive and negative electrodes in a cell, especially in full size batteries, is crucial for optimizing the battery performance [4,5]. These measurements are very important for determining the contribution of the ASI of the individual electrodes to the overall cell ASI.

In this paper, a procedure is described to better understand the electrochemical behavior and limitations of individual electrode by inserting a reference electrode into a commercial size cylindrical Li-ion cell. This approach is also useful in providing the crucial information needed to focus future research efforts to improve and optimize the Li-ion battery performance.

## 2. Experimental

### 2.1. Cell components and assembly

The Li-ion cell used in this study was provided by the Argonne National Laboratory. The cell details are shown in Fig. 1. The positive electrode in this cell consisted of $LiCoO_2$ coated on a thin aluminum foil current collector. The negative electrode was graphite coated on a thin copper foil. Metallic lithium, which has been considered as

* Corresponding author. Tel.: +1-312-567-3639; fax: +1-312-567-8874.

*E-mail address:* prakash@charlie.cns.iit.edu (J. Prakash).

0378-7753/00/$ - see front matter 
PII: S0378-7753(00)00372-4

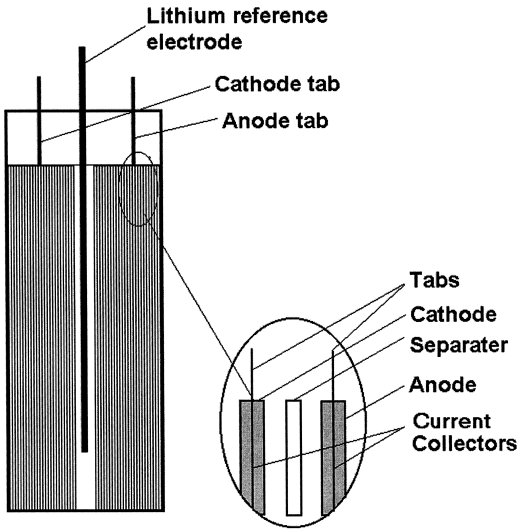


Fig. 1. Schematic diagram of the full size cylindrical Li-ion cell with the reference electrode.

a suitable reference for Li-based redox system [4,5], was used as a reference electrode. The electrolyte composition was 1 M $LiPF_6$ in 1:1 ethylene carbonate (EC)/dimethyl carbonate (DMC). The cell was assembled and operated in an argon atmosphere glove box. The weights of active materials used to coat $LiCoO_2$ cathode and graphite anode were 10.52 and 6.56 g, respectively. The $LiCoO_2$ cathode was the limiting electrode. The weight of the cell was about 30 g. Lithium foil reference electrode was inserted in the center of the cylindrical Li-ion cell. Copper and aluminum foil were used as leads for negative and positive electrodes, respectively. Active areas of the positive and negative electrodes were 518 $cm^2$ and 572 $cm^2$, respectively.

### 2.2. Electrochemical measurements

The three-electrode cell was galvanostatically cycled studied using Arbin Cyclers (ABTS 4.0). The Arbin Cyclers facilitate simultaneous and independent recording of the total cell voltage and the half-cell voltages of both positive and negative electrodes vs. the reference electrode. Unless otherwise specified, the cell was charged at a C-rate to 4.2 V and then trickle charged at 4.2 V for 2.5 h. The cell was subjected to various discharge rates of C, 3C, and 6C in order to compare the performance of the negative and positive electrodes during discharge. The cut-off voltage during the discharge was 2.7 V.

In the static measuring mode, a current interruption technique was used during the cycling to evaluate the electrode and cell impedance. The cell was interrupted for 15 s at every 10% of Depth Of Discharge (DOD). The DC impedance was calculated from the voltage difference during the current interruption interval.

In the dynamic measuring mode, the Partnership for a New Generation of Vehicles (PNGV) Hybrid Pulse Power Characterization (HPPC) test profile [6] was used during the discharge (see Fig. 2). The HPPC test has been designed to investigate the performance of the hybrid vehicle batteries [6]. The HPPC sequence was carried out by first applying an 18-s discharge pulse followed by 32-s rest period. After the rest period, the cell was subjected to a group of regenerative pulses for 10-s (Fig. 2). The cell was subsequently discharged to 10% of capacity at C-rate followed by an hour rest period to allow the cell to return to a charge equilibrium condition before applying the next HPPC sequence. The test is made up of repetition of this profile at various states of discharge. The objective of this test is to estimate the cell impedance from the voltage response curves during discharge, rest and regenerative operation regimes.

### 2.3. Area-specific impedance ($ASI_t$) measurements

The area-specific impedance ($ASI_t$) is time dependent and includes the ohmic, $Li^+$ diffusion through the electrolyte, and solid-state diffusion within the electrode. The ASI measurements were carried out by constant current discharge and current-interruption method. The total measured ASI was resolved into the cathodic and anodic components. A Electrochemical Workstation (CHI, Model 660A) and a Nicolet Oscilloscope (NIC-310) were used for discharge control and current-transient recording to estimate the qualitative values of ohmic and electrochemical components of the total impedance. The cell was galvanostatically cycled at a C-rate with intermittent current interruptions for 15 s. The measured relaxation value of the voltage divided by the current density applied before the current interruption provides the $ASI_{60\ s}$. During the next period of 45-s interruption, a small 11 mV of voltage step was applied with a potentiostat and the current response was recorded with 2 μS data point interval using the oscilloscope. The interruptions and measurements com-

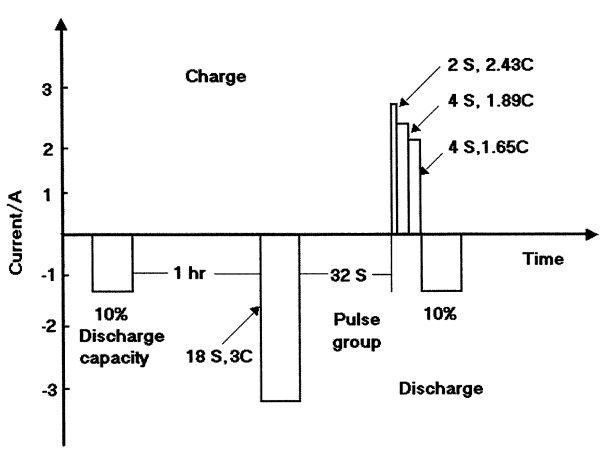


Fig. 2. Hybrid Pulse Power Characterization (HPPC) profile for PNGV.

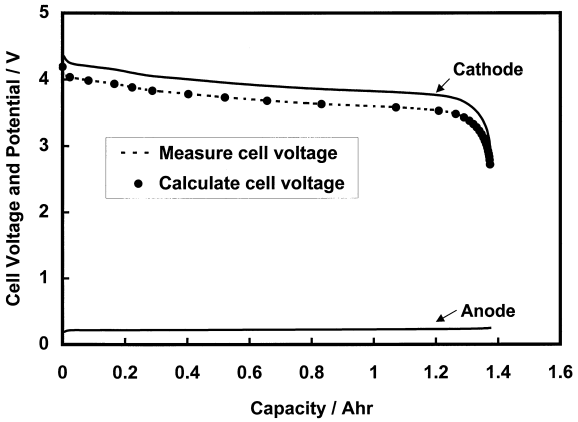


Fig. 3. Voltage profiles of $LiCoO_2$ cathode, graphite anode, and the full cell at C-rate discharge at 25°C.

menced after 10% depth of discharge (DOD) and the sequence was repeated until cell reached 90% of DOD. In order to estimate the individual component contributions to the overall ASI, we also measured the current profile of

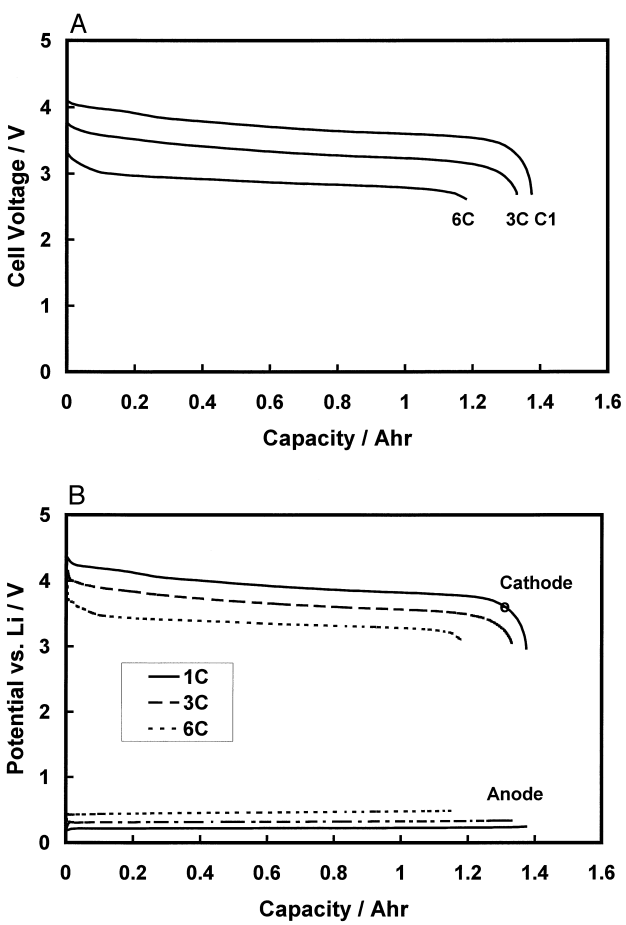


Fig. 4. (A) Discharge voltage curves of Li-ion cell at various discharge rates at 25°C. (B) Discharge voltage curves of $LiCoO_2$ cathode and graphite anode at various discharge rates at 25°C.

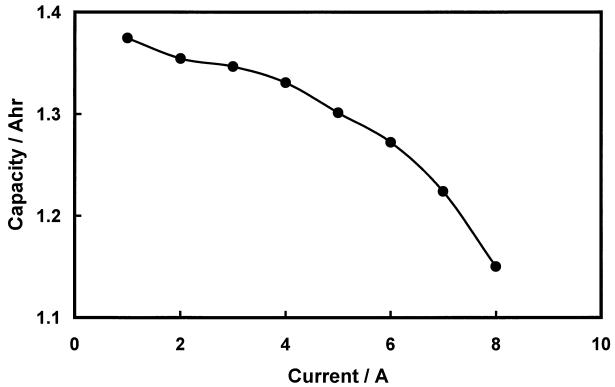


Fig. 5. Effect of discharge rate on the capacity of the Li-ion cell. The cell was discharged to 2.7 V cut-off at 25°C.

the $LiCoO_2$ and the graphite electrode during the 0.5-s small voltage pulses using the potentiostat.

## 3. Results and discussion

### 3.1. Galvanostatic cell cycling

Fig. 3 shows the voltages of the graphite anode and $LiCoO_2$ cathode measured against Li reference electrode in the discharge half-cycle at C-rate. The anode and cathode voltages as well as the overall cell voltage were independently measured in these experiments. The dotted line in Fig. 3 corresponds to the measured true cell voltage. The cell voltage corresponding to the filled circles, on the other hand, was calculated using anode and cathode voltage. It can be seen from this figure that there is negligible difference between the measured and calculated cell voltage indicating the reliability of the measurements.

Typical room temperature cycling behavior of the Li-ion cell and its component electrodes at various discharge rates is shown in Fig. 4A and B. Fig. 4B clearly suggests that the cell capacity is cathode limited. Fig. 5 shows the

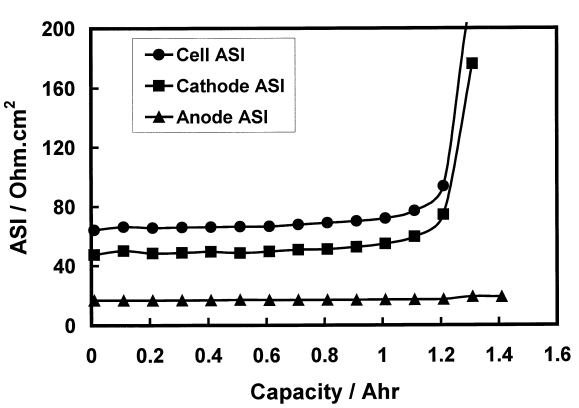


Fig. 6. Area-specific impedance ($ASI_{15\ s}$) of the Li-ion cell and its component electrodes at 25°C. The cell was discharged at a C-rate to 2.7 V.

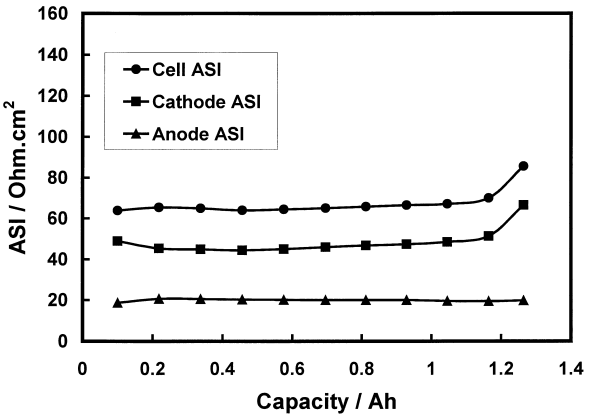


Fig. 7. Area-specific impedance ($ASI_{15\ s}$) of the Li-ion cell and its component electrodes under HPPC test profile with discharge 6 A/18 s pulse.

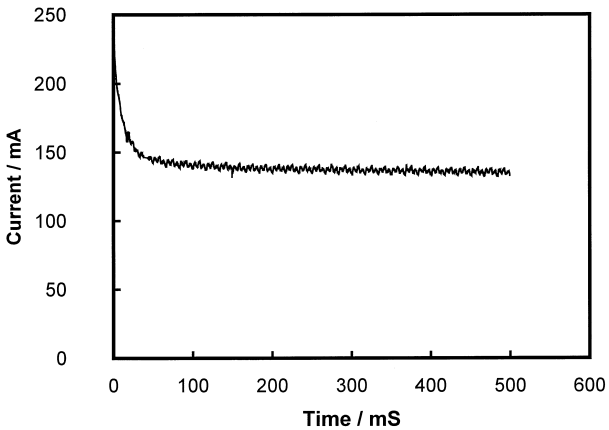


Fig. 9. Cathode current response after an applied 11-mV voltage step.

capacity as a function of the discharge currents. It can be seen from this figure that the cell capacity decrease dramatically as the discharge current is increased beyond 3C rate.

The $ASI_{15\ s}$ were also measured during these tests for the cell and its component electrodes and are shown in Fig. 6. Projections of battery performance based on the ASI measurement of the ASI are highly reliable because this calculation uses the properties that are measured under the actual application conditions. The ASI is time dependent and it includes the ohmic resistance, kinetic and diffusion components of the electrode [7]. The ASI is a very important property of the electrode because it provides information on the nature and magnitude of the electrochemical and mass-transport limitations. The anode and cathode ASI data reported here are not the absolute values but represent the electrode (anode or cathode) and separator. Fig. 6 shows that the ASI for the graphite anode is relatively flat throughout the whole DOD, while the ASIs for the cell and $LiCoO_2$ electrode increase toward the end of discharge. Also, the contribution of the $LiCoO_2$ electrode to the overall cell ASI is about triple of the graphite electrode, but after 80% DOD it rises very sharply (Fig. 6). The lower anode ASI was expected because of good electric conductivity of carbon materials thus lower electric resistance. Moreover, chemical diffusion of Lithium ions in carbon anode materials is generally regarded to be faster than in $LiCoO_2$ [8–10].

### 3.2. Dynamic power performance

A typical behavior of the cell and electrode ASI (under HPPC test) under a 6-A discharge pulse for 18-s duration is shown in Fig. 7. The characteristic features of the dynamic power load ASI curve (Fig. 7) are very similar to the ASI obtained from constant current discharge (Fig. 6). The differences between these curves are a higher anode electrode ASI and somewhat lower cathode ASI in the dynamic power test. The ASI of the $LiCoO_2$ electrode is very similar in both of these tests suggesting that the electrochemical processes taking place at the positive electrode are not significantly affected by the discharge current. However, somewhat lower ASI in HPPC test is

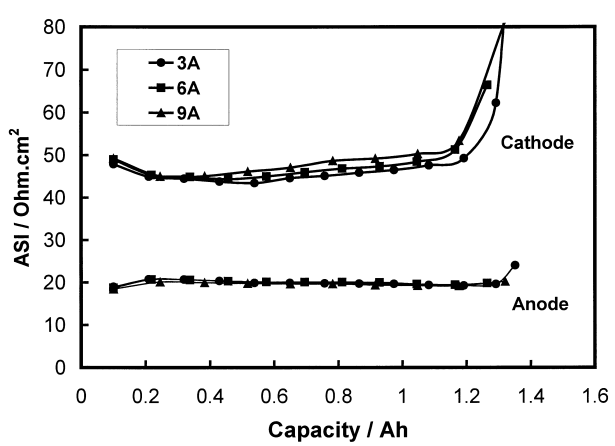


Fig. 8. Effect of discharge current pulses on the area-specific impedance of positive and negative electrodes under HPPC test.

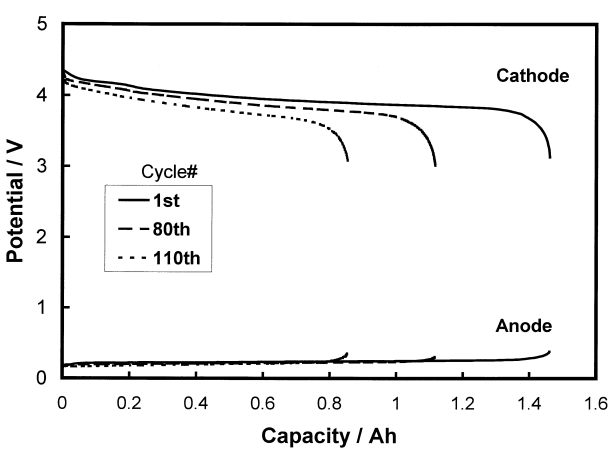


Fig. 10. Electrochemical performance of the cathode and anode as a function of cycle number.

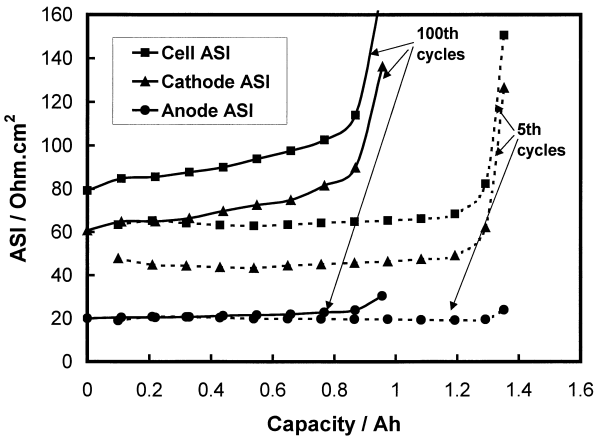


Fig. 11. Effect of cycle number on the area-specific impedance of positive and negative electrodes under HPPC test.

probably associated with temperature increase during the applied pulse [11]. The increased temperature, in turn, decreases the ohmic, kinetic, and diffusion components of ASI producing somewhat lower ASI in HPPC test.

Fig. 8 shows an overall comparison of the electrochemical performance of the negative and positive electrodes under various peak discharge current. It is evident from this figure that the anode ASI did not change under these various peak current levels. However, the cathode ASI showed an increase at higher peak power levels indicating that the electrochemical process at the $LiCoO_2$ electrode and its interface during discharging are strongly dependent on the current level. The increase in the cathode ASI during high dynamic peak power discharge level in the HPPC tests limits the power/energy performance of the Li-ion cell.

### *3.3. Individual component contribution to cathode ASI*

The current-time profile of the $LiCoO_2$ electrode during 0.5-s pulse under an 11-mV discharge voltage step is shown in Fig. 9. It can be seen from this figure that the current changes substantially during first 0.05 s and then reaches a plateau. The change of the current in the first 0.05-s of a 15-s voltage pulse is approximately 60%. Assuming that 0.05-s ASI value is due to the relaxation of the ohmic, kinetic and electrolyte components [7], these results would indicate that these components contribute about 60% in overall power losses.

A representative behavior of this cell after extensive cycling is showed in Fig. 10. A 40% capacity loss after 110 cycles (shown in Fig. 10) can be attributed to the increase in the cell ASI during cycling, dynamic stress cycling, and lack of hermetically sealed cell. The reference electrode cell used in this study could not be hermetically sealed due to the presence of lithium reference electrode. A decrease in the discharge voltage of the cathode was observed with increasing cycle numbers. The deterioration of the $LiCoO_2$ electrode during cycling can be understood by comparing ASI values measured in HPPC test profile at various DOD. As shown in Fig. 11, a large increase in the cell and cathode ASI is clearly evident. The anode ASI, however, remains the same. The increase in the cathode ASI can be attributed to the thicker cathode, non-uniformity of the cathode components (active material, binder, and conductive carbon), de-wetting of the electrode by the electrolyte, and electrode delamination from the current collectors during cycling. In the HPPC test profiles, the upper limit cell voltage was set at 4.5 V at regenerative segment, which may cause overcharge resulting in the decomposition of $LiCoO_2$ [12]. The contaminant such as moisture due to semi-sealed nature of the cell used in this study probably resulted in the formation of lithium oxide and active materials loss at the electrodes [13] during cycling.

## 4. Conclusion

The use of a lithium reference electrode to monitor the commercial size Li-ion cell has been shown to be a powerful technique that reveals the nature of both positive and negative electrode processes during the battery cycling. The cathode was found to be the electrode limiting the power and capacity of the Li-ion cell. The continuous increase of the cathode ASI during cycling also suggests that the $LiCoO_2$ cathode is the primary cause of the energy and power degradation in the LI-ion cells.

## Acknowledgements

This work was supported by the Chemical Technology Division of the Argonne National Laboratory. The authors are grateful to Dr. Khalil Amine and Mr. Gary Henriksen of the Chemical Technology Division, Argonne National Laboratory for encouragement and support. The authors would also like to thank Dr. V.S. Donepudi, Department of Chemical and Environmental Engineering, Illinois Institute of Technology, for reviewing the manuscript and technical comments.

## References

[1] J.J. Auborn, Y.L. Barberio, J. Electrochem. Soc. 134 (1987) 639.
[2] T. Naguara, K. Tazawa, Prog. Batteries Sol. Cells 9 (1990) 20.
[3] S.L. Wilkinson, Chem. Eng. News 75 (41) (1997) 18.
[4] A. Blyr, C. Sigala, G. Amatucci, D. Guyomard, Y. Chabre, J.-M. Tarascon, J. Electrochem. Soc. 145 (1998) 194.
[5] C.G. Thurston, J.R. Owen, J. Power Sources 39 (1992) 215.
[6] Idaho National Engineering Laboratory, PNGV Battery Test Manual, Revision1, DOE/ID-10597, 1998.

[7] L. Redey, D.R. Vissers, J. Newman, S. Higuchi, in: H.C. Maru (Ed.), Proc. Symp. On Porous Electrodes: Theory and Practice Vols. 74–78 The Electrochemical Society, Pennington, NJ, 1984, pp. 322–335.
[8] N. Takami, A. Satoh, M. Hara, T. Ohsaki et al., J. Electrohem. Soc. 142 (1995) 371.
[9] A. Honders, J.M. der Kinderen, A.H. van Heeren, J.H.W. de Wit, G.H.J. Broers, Solid State Ionics 15 (1985) 265.
[10] K. Mizushima, P.C. Jones, P.J. Wiseman, J.B. Goodenough, Solid State Ionics 3–4 (1981) 171.
[11] J. Liu, A.N. Jansen, K. Kepler, A. Newman, G.L. Henriksen, K. Amine, in: The Meeting Abstract of 195th Electrochemical Society Vols. 99–911999, No.52.
[12] G.G. Amatucci, J.M. Tarascon, L.C. Klien, Solid State Ionics 83 (1996) 167.
[13] P. Arora, R.E. White, J. Electrochem. Soc. 145 (1998) 3647.